The Dark Energy Survey Supernova Program: an updated measurement of the Hubble constant using the inverse distance ladder

R. Camilleri [1]★ T. M. Davis [1] S. R. Hinton [1] P. Armstrong,[2] D. Brout,[3] L. Galbany [4,5]
K. Glazebrook,[6] J. Lee [7] C. Lidman [2,8] A. Möller,[6] R. C. Nichol,[9] M. Sako,[7] D. Scolnic,[10] P. Shah,[11]
M. Smith,[12] M. Sullivan,[12] B. O. Sánchez,[10,13] M. Vincenzi,[10] P. Wiseman,[12] S. Allam,[14] T. M.
C. Abbott,[15] M. Aguena,[16] F. Andrade-Oliveira,[17] J. Asorey,[18] S. Avila,[19] D. Bacon,[20] K. Bechtol,[21]
S. Bocquet,[22] D. Brooks,[11] E. Buckley-Geer,[14,23] D. L. Burke,[24,25] A. Carnero Rosell,[16,26] D. Carollo,[27]
J. Carretero,[19] F. J. Castander,[4,5] C. Conselice,[28,29] L. N. da Costa,[16] M. E. S. Pereira,[30] S. Desai,[31] H.
T. Diehl,[14] S. Everett,[32] I. Ferrero,[33] B. Flaugher,[14] J. Frieman,[14,34] J. García-Bellido,[35] E. Gaztanaga,[4,5,20]
G. Giannini,[19,34] R. A. Gruendl,[36,37] K. Herner,[14] D. L. Hollowood,[38] K. Honscheid,[39,40] D. Huterer,[17] D.
J. James,[3] S. Kent,[14,34] K. Kuehn,[41,42] O. Lahav,[11] S. Lee,[32] G. F. Lewis,[43] M. Lima,[16,44] J. L. Marshall,[45]
J. Mena-Fernández,[46] R. Miquel,[19,47] J. Myles,[48] R. L. C. Ogando,[49] A. Palmese,[50] A. Pieres,[16,49] A.
A. Plazas Malagón,[24,25] A. K. Romer,[51] A. Roodman,[24,25] S. Samuroff,[52] E. Sanchez,[53] D. Sanchez Cid,[53]
M. Schubnell,[17] I. Sevilla-Noarbe,[53] E. Suchyta,[54] N. Suntzeff,[45] M. E. C. Swanson,[36] G. Tarle,[17] B.
E. Tucker,[2] A. R. Walker,[15] and N. Weaverdyck[55,56] (DES Collaboration)

Affiliations are listed at the end of the paper

ABSTRACT

We measure the current expansion rate of the Universe, Hubble's constant H_0, by calibrating the absolute magnitudes of supernovae to distances measured by baryon acoustic oscillations (BAO). This 'inverse distance ladder' technique provides an alternative to calibrating supernovae using nearby absolute distance measurements, replacing the calibration with a high-redshift anchor. We use the recent release of 1829 supernovae from the Dark Energy Survey spanning $0.01 < z < 1.13$ anchored to the recent baryon acoustic oscillation measurements from Dark Energy Spectroscopic Instrument (DESI) spanning $0.30 < z_{\mathrm{eff}} < 2.33$. To trace cosmology to $z = 0$, we use the third-, fourth-, and fifth-order cosmographic models, which, by design, are agnostic about the energy content and expansion history of the universe. With the inclusion of the higher redshift DESI-BAO data, the third-order model is a poor fit to both data sets, with the fourth-order model being preferred by the Akaike Information Criterion. Using the fourth-order cosmographic model, we find $H_0 = 67.19^{+0.66}_{-0.64}$ km s^{-1} Mpc^{-1}, in agreement with the value found by Planck without the need to assume Flat-ΛCDM. However, the best-fitting expansion history differs from that of Planck, providing continued motivation to investigate these tensions.

Key words: cosmological parameters – distance scale – cosmology: observations.

1 INTRODUCTION

Resolving the tension between late-time and early-time measurements of the Hubble constant (H_0) is one of the most significant challenges presented by the standard cosmological model. The Planck Collaboration (hereafter Planck; Aghanim et al. 2020), which measures the cosmic microwave background (CMB) radiation, estimates the local expansion rate to be $H_0 = 67.4 \pm 0.5$ km s^{-1} Mpc^{-1} assuming a spatially flat ΛCDM (cold dark matter) universe. This value is in $\sim 5\sigma$ tension and substantially lower than that determined

by the SH0ES collaboration (Riess et al. 2022), $H_0 = 73.04 \pm 1.04$ km s^{-1} Mpc^{-1} using a distance ladder consisting of Cepheid calibrated supernova (SN) luminosity distances from Pantheon+ (Brout et al. 2022; Scolnic et al. 2022), assuming only the cosmological principle, that is our universe is homogeneous and isotropic at large scales. For a recent review of the Hubble constant, see Shah, Lemos & Lahav (2021).

The discrepancy between early and late-time measurements might imply new physics and has resulted in alternate cosmological models being proposed. Recent investigations into alternate models have shown many to be compatible with various data sets (Dam, Heinesen & Wiltshire 2017; Zhang, Li & Xia 2017; Camilleri et al. 2024). There also might be unaccounted for systematics or some unknown

★ E-mail: uqrcamil@uq.edu.au

physical phenomenon that has not been taken into account in the current models of the universe's expansion and has motivated an increase in new, independent ways to determine H_0.

Since SN Ia are relative distance indicators, their observed magnitude must be calibrated using an absolute distance measurement. In the distance ladder approach used by SH0ES, parallax measurements to nearby Cepheid variable stars are used to calibrate the luminosities of SNe Ia. Therefore, one alternate way to determine H_0 involves replacing Cepheids as calibrators for SNe Ia, avoiding unknown systematics associated with this specific method. Freedman (2021) and Anand et al. (2022) calibrate the SN Ia with tip of the red giant branch (TRGB) distances to host galaxies, and found $H_0 = 69.8 \pm 0.6$ (stat) ± 1.6 (sys) km s^{-1} Mpc^{-1} and $H_0 = 71.5 \pm 1.8$ km s^{-1} Mpc^{-1} respectively, both consistent to within 2σ of the SH0ES result. Recently, Scolnic et al. (2023) also calibrated the SNe Ia with TRGB distances and measured a higher value finding $H_0 = 73.22 \pm 2.06$ km s^{-1} Mpc^{-1}. For more details and a review on recent TRGB measurements see Li & Beaton (2024). Surface brightness fluctuations (SBF) of a host galaxy can also be used to calibrate SNe Ia (Tonry & Schneider 1988; Blakeslee, Ajhar & Tonry 1999; Biscardi et al. 2008; Blakeslee et al. 2009). This technique was first used by Khetan et al. (2021), who found $H_0 = 70.50 \pm 2.37$ (stat) ± 3.38 (sys) km s^{-1} Mpc^{-1}, consistent with the value obtained by SH0ES and Planck. A later measurement by Garnavich et al. (2023) found a higher value of $H_0 = 74.6 \pm 0.9$ (stat) ± 2.7 (sys) km s^{-1} Mpc^{-1}. Blake et al. (2011) also show that SN can be used with the Alcock–Paczynski test to measure the cosmic history in a model-independent way and determined $H(z)/[H_0(1 + z)]$ in four different redshift slices to $10 - 15$ per cent accuracy.

The approach we take here is to use the inverse distance ladder method where the observed magnitudes of SNe Ia are calibrated using distance measurements from baryon acoustic oscillations (BAOs) with a prior on the CMB sound horizon at the time of photon-baryonic decoupling after recombination. We then use the cosmographic approach (Aubourg et al. 2015; Macaulay et al. 2019), which is a smooth Taylor expansion of $H(z)$ (see Section 2.1) to theoretically trace the cosmology to $z = 0$ assuming a FLRW metric and the Etherington distance duality relation[1] (Etherington 1933).

This procedure was first used by Aubourg et al. (2015), who found $H_0 = 67.3 \pm 1.1$ km s^{-1}Mpc^{-1} in agreement with the Planck result using 740 SNe Ia from the joint light-curve analysis (Betoule et al. 2014, hereafter JLA) and BAO measurements from the Baryon Oscillation Spectroscopic Survey (BOSS) Data Release Eleven (DR11; Anderson et al. 2014).

Harnessing the same technique, Macaulay et al. (2019) found $H_0 = 67.8 \pm 1.3$ km s^{-1} Mpc^{-1} using 207 SN Ia from the Dark Energy Survey (DES) Collaboration's (Abbott et al. 2019) 3-yr SN release, with BAO measurements taken from Carter et al. (2018) and the Baryon Oscillation Spectroscopic Survey Data Release Twelve (BOSS DR12; Alam et al. 2017).

Recently, DES has released the largest single sample of SNe to date. The release consisted of 1829 SNe in the redshift range $0.01 < z < 1.13$ (DES Collaboration 2024). Furthermore, the Dark Energy Spectroscopic Instrument (DESI) team (DESI Collaboration et al. 2024) has provided BAO measurements in seven redshift bins from over 6 million extragalactic objects in the redshift range $0.1 < z < 4.2$. In this paper, we use these data sets from both DES and DESI

to provide an updated measurement of H_0 using the inverse distance ladder technique.

This paper is organized as follows, in Section 2 we provide the basic theory, methodology and data sets used in our analysis. We present our results in Section 3 and conclude in Section 4.

2 METHODOLOGY AND DATA

2.1 Cosmographic expansion

To trace the cosmology to $z = 0$, we use the well-established cosmographic expansion, which is a smooth Taylor expansion of the scale factor a that makes minimal assumptions about the underlying cosmological model but retains the assumptions of homogeneity and isotropy (Visser 2004; Zhang et al. 2017). Here, we note the definition of the deceleration parameter,

$$q = -\frac{1}{H^2}\frac{1}{a}\frac{d^2a}{dt^2}, \qquad (1)$$

the jerk parameter,

$$j = \frac{1}{H^3}\frac{1}{a}\frac{d^3a}{dt^3}, \qquad (2)$$

the snap parameter,

$$s = \frac{1}{H^4}\frac{1}{a}\frac{d^4a}{dt^4}, \qquad (3)$$

and the lerk parameter,

$$l = \frac{1}{H^5}\frac{1}{a}\frac{d^5a}{dt^5}. \qquad (4)$$

With these definitions, the Hubble parameter can be expressed to fifth-order as,

$$H(z) = H_0\left[1 + \mathcal{H}_1 z + \mathcal{H}_2 z^2 + \mathcal{H}_3 z^3 + \mathcal{H}_4 z^4\right], \qquad (5)$$

where

$$\mathcal{H}_1 = (1 + q_0),$$
$$\mathcal{H}_2 = \frac{1}{2}\left(j_0 - q_0^2\right),$$
$$\mathcal{H}_3 = \frac{1}{6}\left(3q_0^2 + 3q_0^3 - 4q_0 j_0 - 3j_0 - s_0\right),$$
$$\mathcal{H}_4 = \frac{1}{24}(-12q_0^2 - 24q_0^3 - 15q_0^4 + 32q_0 j_0 + 25q_0^2 j_0$$
$$+ 7q_0 s_0 + 12j_0 - 4j_0^2 + 8s_0 + l_0),$$

and q_0, $j_0 s_0$, and l_0 are the current epoch deceleration, jerk, snap, and lerk parameters, respectively. The luminosity distance, $D_L(z)$ for a spatially flat universe is given by,

$$D_L(z) = z + \mathcal{D}_1 z^2 + \mathcal{D}_2 z^3 + \mathcal{D}_3 z^4 + \mathcal{D}_4 z^5, \qquad (6)$$

where

$$\mathcal{D}_1 = \frac{1}{2}\left(1 - q_0\right),$$
$$\mathcal{D}_2 = -\frac{1}{6}\left(1 - q_0 - 3q_0^2 + j_0\right),$$
$$\mathcal{D}_3 = \frac{1}{24}\left(2 - 2q_0 - 15q_0^2 + 5j_0 + 10q_0 j_0 + s_0\right),$$
$$\mathcal{D}_4 = \frac{1}{120}(-6 + 6q_0 + 81q_0^2 + 165q_0^3 + 105q_0^4 + 10j_0^2$$
$$- 27j_0 - 110q_0 j_0 - 105q_0^2 j_0 - 15q_0 s_0 - 11s_0 - l_0).$$

---

[1]The Etherington distance duality relates the luminosity distance $D_L(z)$ to the angular diameter distance $D_A(z)$ by $D_L(z) = D_A(z)(1 + z)^2$.

2.2 DES-SN5YR

In this analysis, we use the DES-SN5YR sample containing 1829 likely SNe Ia. The DES-SN5YR sample is the largest and deepest single sample survey to date consisting of 1635 SNe Ia-like candidates ranging in redshift from 0.05 to 1.13 from the DES survey with 1499 photometrically classified as type Ia SNe using the open-source algorithm SUPERNNOVA (Möller et al. 2022). The sample from DES is complemented by 194 spectroscopically confirmed low-redshift SN Ia. For more details see Vincenzi et al. (2024) and Sánchez et al. (2024).

The DES-SN5YR Hubble diagram[2] includes corrected SN apparent magnitudes, distance moduli (calculated using an assumed H_0 of 70), heliocentric redshifts, CMB corrected redshifts, and redshifts with both CMB and peculiar velocity corrections. The DES Hubble diagram is ideal to constrain the history of the cosmic expansion rate. However, as the SN are not anchored to a specific calibrator, on its own, it offers little information regarding H_0 or the SN Ia peak absolute magnitude, M_B due to a degeneracy between these parameters. However, this degeneracy can be broken with BAO data and therefore we use the *corrected* apparent magnitudes provided by DES and calculate our data vector as,

$$\mu_{\text{data}}(M_B) = m_{b,\text{data}} - M_B, \tag{7}$$

where M_B is a free parameter. The distance moduli can then be calculated as,

$$\mu_{\text{theory}}(z, \Theta) = 5\log_{10}[D_L(z, \Theta)/1 \text{ Mpc}] + 25, \tag{8}$$

where $D_L(z, \Theta)$ is given in equation (6) and depends on the set of cosmological parameters, Θ. In this analysis, we fit cosmographic expansion three ways: to third-order [equation (6) excluding the z^4 and z^5 terms], fourth-order [equation (6) excluding the z^5 term] and fifth-order (equation 6) with $\Theta = \{H_0, q_0, j_0\}$, $\Theta = \{H_0, q_0, j_0, s_0\}$, and $\Theta = \{H_0, q_0, j_0, s_0, l_0\}$, respectively.

We compute the difference between data and theory for every ith SN, $D_i(M_B, \Theta) = \mu_{\text{data}}(M_B) - \mu_{\text{theory}}(z, \Theta)$, and find the minimum of the χ^2 likelihood given by,

$$-2\ln(\mathcal{L}) = \chi^2_{\text{SN}}(M_B, \Theta) = \vec{\mathbf{D}}^T \mathbf{C}_{\text{SN}}^{-1} \vec{\mathbf{D}}, \tag{9}$$

where $\mathcal{C}_{\text{SN}}^{-1}$ is the inverse covariance matrix including both statistical and systematic errors.[2]

2.3 DESI-BAO

The sound horizon at the time of baryon decoupling in the early universe, i.e. the drag epoch (at $z \simeq 1060$), left an imprint in the distribution of matter, which is detectable in the galaxy distribution. These BAO serve as cosmological standard rulers (Blake & Glazebrook 2003; Linder 2003; Seo & Eisenstein 2003; McDonald & Eisenstein 2007; Alam et al. 2017; DESI Collaboration 2024). In this work, we use measurements of the BAO provided by the DESI collaboration (DESI Collaboration 2024). The DESI-BAO provide twelve measurements in seven redshift bins from over 6 million extragalactic objects in the redshift range $0.1 < z < 4.2$.

BAO measurements have a physical scale set by the sound horizon, r_s at the end of the drag epoch, $r_d \equiv r_s(z_*)$, and are observed from pairs of galaxies averaged over all angles. Measurements are generally quoted as $D_H(z)/r_d$ for separation vectors of the pairs

that are oriented parallel to the line of sight and $D_M(z)/r_d$ for pairs oriented perpendicular to the line of sight with both results being correlated. For certain redshift bins with low signal-to-noise ratio, the volume-averaged quantity $D_V(z)/r_d$ is quoted. The distances $D_H(z)$, $D_M(z)$ are the Hubble and transverse comoving distances, respectively, and can be calculated as,

$$D_H(z, \Theta) = c/H(z, \Theta), \tag{10}$$

where $H(z, \Theta)$ is given in equation (5) and

$$D_M(z, \Theta) = D_L(z, \Theta)/(1 + z_{\text{obs}}), \tag{11}$$

where z is the redshift due to the expansion of the Universe, z_{obs} is the observed redshift and $D_L(z, \Theta)$ is given in equation (6). The dilation scale, $D_V(z)$ is a combination of the two distances and defined as,

$$D_V(z, \Theta) \equiv \left[zD_M^2(z, \Theta)D_H(z, \Theta) \right]^{1/3}. \tag{12}$$

Lastly, we require knowledge of r_d, which depends on the baryon density and total matter density in the early universe. In this work we adopt a Gaussian prior of $r_d \sim \mathcal{N}(147.46, 0.28)$ Mpc determined using constraints from Lemos & Lewis (2023), who removed late-time cosmology dependence from the CMB likelihoods (Planck Flat-ΛCDM) associated with modelling the late-integrated Sachs–Wolfe (late-ISW) effect, the optical depth to re-ionization, CMB lensing, and foregrounds. This was done by using empirical measurements of the CMB lensing reconstruction, combined with weak priors on the smoothness of the lensing spectrum, foregrounds, and shape of any additional late-ISW effect.

To constrain the DESI-BAO data we find the minimum of

$$\chi^2_{\text{BAO}}(r_d, \Theta) = \vec{\Delta}^T \mathbf{C}_{\text{BAO}}^{-1} \vec{\Delta}, \tag{13}$$

where $\Delta(r_d, \Theta)$ is the difference between the measurements and the associated values determined with the cosmographic model and $\mathcal{C}_{\text{BAO}}^{-1}$ is the inverse covariance matrix provided with the DESI-BAO.

2.4 Fitting for H_0

To determine H_0 using the inverse distance ladder technique, we perform a combined fit to the DES-SN5YR and DESI-BAO, breaking the degeneracy between M_B and H_0. The likelihoods are combined as,

$$\chi^2_{\text{tot}}(M_B, r_d, \Theta) = \chi^2_{\text{BAO}}(r_d, \Theta) + \chi^2_{\text{SN}}(M_B, \Theta) \tag{14}$$

and minimized using the dynamic nested sampling package, `Dynesty` (Skilling 2004; Skilling 2006; Higson et al. 2018; Speagle 2020; Koposov et al. 2023) with 500 live points. We also used `Dynesty`'s inbuilt stopping function, which decides when to stop sampling based on a posterior and evidence error threshold, with the default values.

3 RESULTS AND DISCUSSION

To validate the pipeline we generated 100 mocks of SN+BAO data prior to fitting and ensured we were able to recover our input cosmology. For our SN and BAO mocks, we drew realizations centred on distances determined using $\{M_B, r_d, H_0, q_0, j_0, s_0\} = \{-19.5, 147, 68, -0.55, -0.8, -0.95\}$ as a fiducial cosmology and used a correlated Gaussian distribution with the covariance given by the covariance matrices of the DES-SN5YR and DESI-BAO data to ensure a realistic dispersion. After this validation, the pipeline was frozen, with the exception of what prior to use on the sound horizon. Initially, we used the prior from the Planck CMB constraint of

---

[2]Available at https://github.com/des-science/DES-SN5YR along with the statistical+systematic covariance matrix used in this analysis.

Table 1. Best-fitting parameters determined with the combined DES-SN5YR+DESI-BAO data sets. These results are the medians of the marginalized posterior with 68.27 per cent integrated uncertainties. The ΔAIC with respect to the fourth-order cosmographic model ($\chi^2 = 1692$) is quoted in the final column.

Model	H_0	M_B	Ω_m	q_0	j_0	s_0	l_0	ΔAIC
Flat-ΛCDM	$67.67^{+0.69}_{-0.68}$	$-19.394^{+0.017}_{-0.016}$	0.322 ± 0.012	–	–	–	–	6.1
Third order	$70.03^{+0.66}_{-0.65}$	$-19.344^{+0.016}_{-0.015}$	–	-0.551 ± 0.025	$0.703^{+0.056}_{-0.057}$	–	–	89.9
Fourth order	$67.19^{+0.66}_{-0.64}$	$-19.375^{+0.018}_{-0.017}$	–	-0.342 ± 0.013	$0.255^{+0.087}_{-0.091}$	$-0.494^{+0.046}_{-0.048}$	–	0.0
Fifth order	$67.26^{+0.73}_{-0.71}$	-19.381 ± 0.018	–	$-0.391^{+0.032}_{-0.033}$	$0.539^{+0.031}_{-0.030}$	$-0.45^{+0.32}_{-0.30}$	$2.6^{+1.1}_{-1.2}$	2.3

$r_d = 147.05 \pm 0.30$ (Aghanim et al. 2020) however, this choice has minimal impact on our results and does not change our conclusions (we provide the best-fitting H_0 using this prior below).

Best-fitting parameters determined with the combined DES-SN5YR+DESI-BAO data sets are shown in Table 1 and Fig. 1. We plot the best-fitting expansion histories in the top right of Figs 1 and 2. These results are the medians of the marginalized posterior with 68.27 per cent integrated uncertainties determined with the 'cumulative' option in the Python package ChainConsumer (Hinton 2016).

To assess whether the additional parameters used in the higher order cosmographic models are required given the data we use the Akaike Information Criterion AIC $\equiv 2k - 2\ln \mathcal{L}^{max}$ (Akaike 1974), where k is the number of parameters in the model. In the final column of Table 1 we quote the ΔAIC relative to the fourth-order cosmographic model. To assess the strength for or against a model, Trotta (2008) suggests that $\Delta > 2$, $\Delta > 5$, and $\Delta > 10$ indicates weak, moderate, and strong evidence respectively, against the model with the higher Δ value.

We find strong evidence against the third-order cosmographic model with ΔAIC $= 89.9$ that is driven by the model's poor fit to both data sets with a $\Delta\chi^2 = 81$ relative to the fourth-order cosmographic model. For reference, we include the flat-ΛCDM fit. This result shows that the fourth-order model is a good fit to the data and is moderately preferred over flat-ΛCDM (ΔAIC $= 6.1$). Note that the third-order cosmographic model has been shown to be a good fit to the DES-SN5YR alone (although fourth order is still preferred by AIC; see Camilleri et al. 2024). However, with the inclusion of the higher redshift DESI data, a more flexible model is needed. We therefore do not discuss the third-order model any further. Both of our key results, presented below, are quoted using the fourth-order cosmographic expansion. However, we note that there is no preference for or against the fourth- and fifth-order expansions based on the AIC. This choice does not impact the conclusions of this paper with both models giving consistent constraints on H_0.

The combined DES-SN5YR+DESI-BAO data sets yield $H_0 = 67.19^{+0.66}_{-0.64}$ km s^{-1} Mpc^{-1}(median of the marginalized posterior with 68.27 per cent integrated uncertainties) when using the fourth-order cosmographic model. This measurement is consistent with the Planck+Flat-ΛCDM measurement of $H_0 = 67.4 \pm 0.5$ km s^{-1} Mpc^{-1} (Aghanim et al. 2020), previous inverse distance ladder measurements from Aubourg et al. (2015) and Macaulay et al. (2019), who found $H_0 = 67.3 \pm 1.1$ and $H_0 = 67.8 \pm 1.3$ km s^{-1} Mpc^{-1}, respectively (see Fig. 3) and Mukherjee & Sen (2024) who use Gaussian process regression to reconstruct the expansion history and constrain $H_0 r_d$ using the DES-SN5YR+DESI-BAO data sets, finding $H_0 r_d = 9930.09^{+22.78}_{-22.91}$. The Macaulay et al. (2019) H_0 measurement was also determined using the fourth-order cosmographic model. However, the uncertainties in our measurement are smaller by ~ 50 per cent, highlighting the advancements in constraining power from both the DES-SN5YR+DESI-BAO data

sets. Our measurement is inconsistent at $\sim 4.6\sigma$ to the SH0ES collaboration measurement of $H_0 = 73.04 \pm 1.04$ km s^{-1} Mpc^{-1} (Riess et al. 2022) determined with the local distance ladder.

Repeating the analysis with only the statistical uncertainties included in the supernova data covariance matrix, we find the statistical only uncertainty $\sigma_{stat} = 0.59$. Defining the systematic only uncertainty as

$$\sigma_{sys} = \sqrt{\sigma_{stat+sys}^2 - \sigma_{stat}^2}, \tag{15}$$

we find $\sigma_{sys} = 0.28$. For a further breakdown of the systematics, including which uncertainties are now the dominant contributors to the error budget within the DES-SN5YR sample, see Vincenzi et al. (2024).

We find $M_B = -19.375^{+0.018}_{-0.017}$, which is lower than the value quoted by the SH0ES collaboration of $M_B = -19.253 \pm 0.027$, using Cepheid calibrated SNe Ia. We note that our value is significantly lower than the value quoted by Macaulay et al. (2019) and Aubourg et al. (2015), who both find $M_B \approx -19.1$[3] However, our result is in agreement with various other works who calibrate SN with high redshift data (Camarena & Marra 2020, 2023; Dinda & Banerjee 2023).

We see that the expansion history of the SNe does not vary enough to recover a high H_0 given that we have anchored the SNe to the BAO scale, which was in turn calibrated to the CMB values of the sound horizon at the drag epoch, r_d. It is clear from Fig. 2 that although the SNe do prefer a higher H_0, once the BAO have set the absolute scale on the vertical axis of $c \ln(1 + z)/D_M(z)$, then it is very difficult for the supernovae to change the shape of the expansion history sufficiently to recover a H_0 (y-intercept of Fig. 2) above 70 km s^{-1} Mpc^{-1}. To clarify, we find that the shape of the supernova Hubble diagram is consistent with the shape of the BAO Hubble diagram. Importantly, our findings show that the magnitude offset of the supernova Hubble diagram can be calibrated using the low-z distance ladder or calibrated using higher-z BAO, but not both simultaneously. Our results do not say which calibration is correct, just that the calibrations are inconsistent and the shape of the Hubble diagram below $z = 2.5$ cannot solve the inconsistency.

We note that our assumed prior on the sound horizon is consistent with the Planck CMB measurement of $r_d = 147.05 \pm 0.30$ (Aghanim et al. 2020). Repeating the analysis with this value yields a consistent constraint on H_0 of $67.36^{+0.68}_{-0.64}$ km s^{-1} Mpc^{-1} ($\Delta H_0 = 0.17$). We also perform two additional tests. First, we test the

---

[3]Prior to this analysis, we attempted to replicate the results of Macaulay et al. (2019). We recovered a best fit $H_0 = 67.5^{+1.2}_{-1.1}$ km s^{-1} Mpc^{-1} consistent with the value that they quote, however we find $M_B = -19.415 \pm 0.027$, which is consistent with the best-fitting M_B found in this work using the DES-SN5YR+DESI-BAO. It is our opinion that the value of M_B in Macaulay et al. (2019) may have been misquoted.
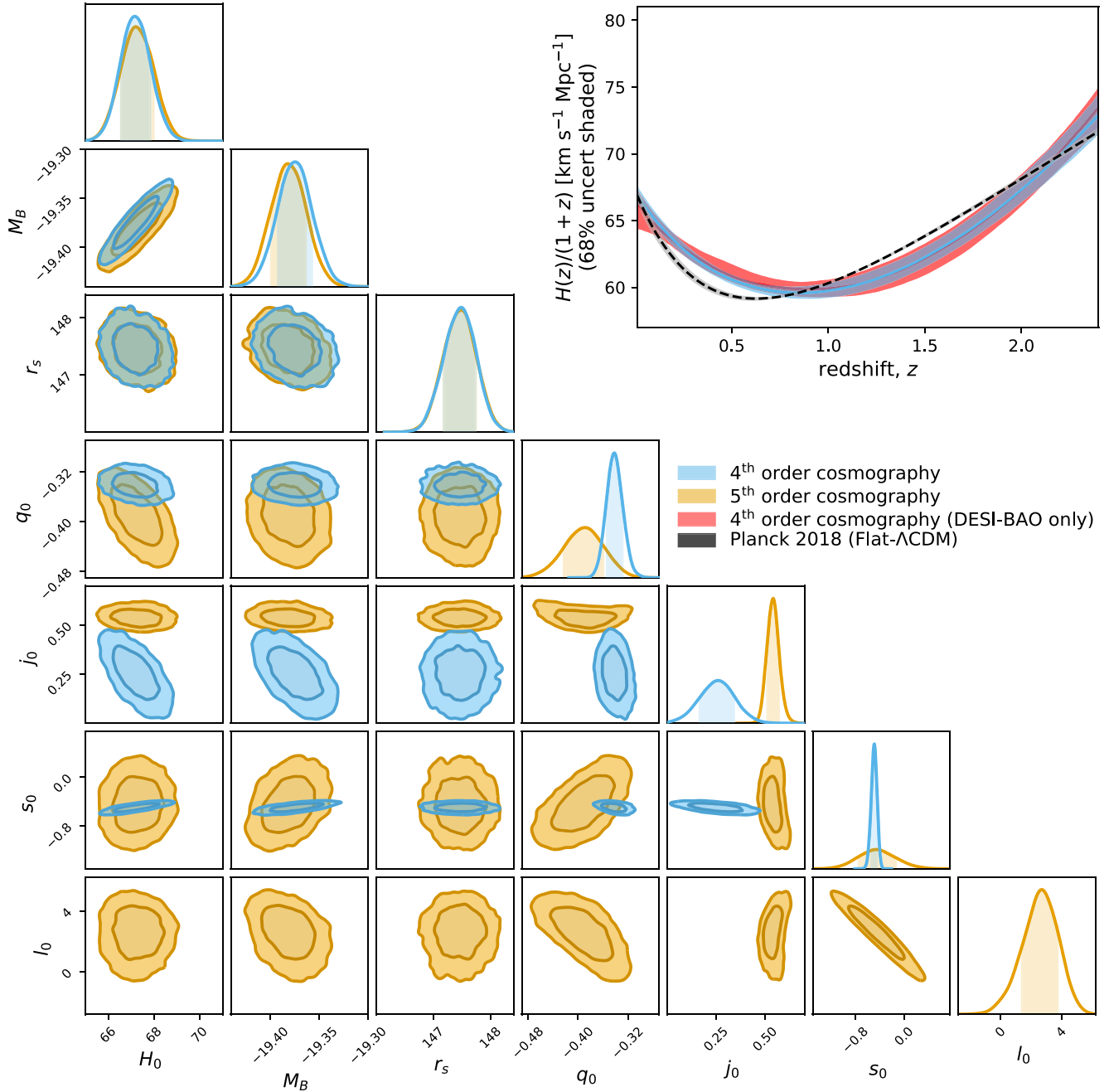
Figure 1. The constraints on H_0, M_B, r_s, and the fourth (blue) and fifth (orange) order cosmographic parameters using the combined DES-SN5YR+DESI-BAO data sets. Contours represent the 68.3 per cent and 95.5 per cent confidence intervals. The median of the marginalized posterior and cumulative 68.27 per cent confidence intervals are given in Table 1. In the top right of the figure, we also present the best-fitting expansion history for the fourth-order cosmographic model (blue) determined with the DES-SN5YR+DESI-BAO data sets. For comparison, we include the expansion history from Planck, which was determined by analysing the CMB and assuming Flat-ΛCDM (black dashed line) and the fourth-order cosmographic model fit to the DESI-BAO alone (red).

sensitivity of our constraint on H_0 to a ±2σ shift in the central value of our prior on r_d and find $|\Delta H_0| < 0.27$. Secondly, we fix $H_0 = 73$ and instead fit for the sound horizon finding $r_d = 135.7 \pm 1.3$. This result shows we would need to shift r_d by ~ 10 to recover the SH0ES H_0 value and casts the H_0 tension in terms of a sound horizon tension, as discussed in Aylor et al. (2019).

Here, the supernova data are adding a more detailed expansion history constraint at mid-redshift to low-redshift than the BAO provide. Fig. 1 compares the expansion histories of the fourth-

order cosmography fit using DESI-BAO alone and that of the fit to the combined DES-SN5YR + DESI-BAO, demonstrating the improvement in constraining power from the combination of data sets. Both expansion histories differ from that of Planck, which assumes flat-ΛCDM, but agree with each other. This is in line with the interesting result that DESI-BAO and DES-SN5YR found consistent non-ΛCDM expansion histories when fitting for a model that allowed time-varying dark energy (Flat-w_0w_aCDM, see DES Collaboration 2024; DESI Collaboration 2024).
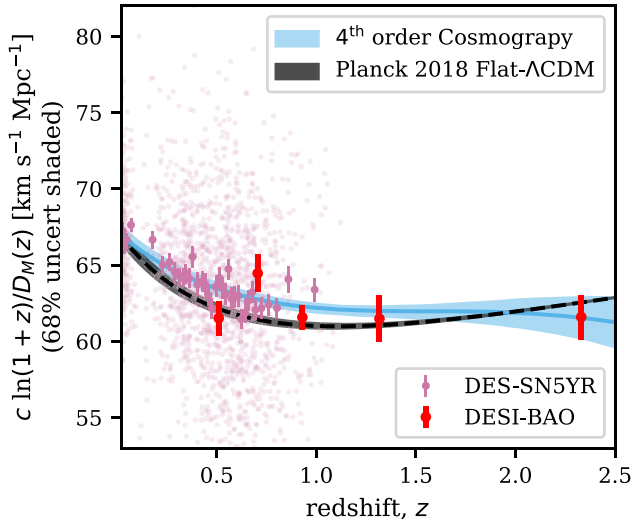
Figure 2. Illustration of the inverse distance ladder method. The pink supernova data points from DES-SN5YR have been calibrated to the red data points from DESI-BAO, and the resulting y-intercept gives H_0. For DESI-BAO we plot only the five $D_M(z)/r_d$ points and their statistical uncertainties. For the DES-SN5YR sample we show both the individual SN events (transparent) and the redshift-binned SN distance moduli (opaque with redshift-binned statistical uncertainties) after calibration. We show the redshift-binned SN for visualization only. We calculate the binned points using the average-weighted mean, the uncertainties are the standard error of the mean, and we ensure each bin has approximately 50 SN. The blue line represents the best-fitting fourth-order cosmographic model determined with the DES-SN5YR+DESI-BAO data sets. The black dashed line shows the best fit from Planck (Aghanim et al. 2020), determined by analysing the CMB and assuming Flat-ΛCDM.
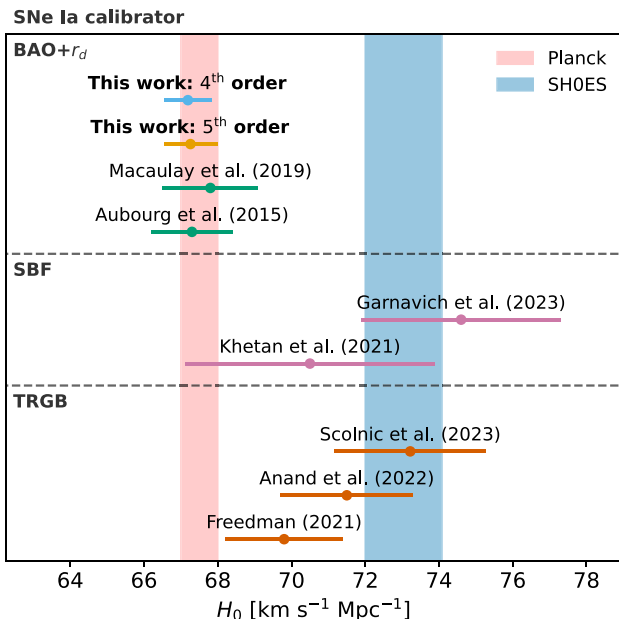
Figure 3. A comparison of Hubble constant values using different SNe Ia calibrators and the results from this work for the fourth- (blue) and fifth- (orange) order cosmographic fit. The red shaded regions represent the 68 per cent confidence interval for the Planck (red) and SH0ES (blue) result.

In Fig. 3 we compare our result for H_0 with other results in the literature. The result we present here is the first inverse distance ladder measurement that has an uncertainty on H_0 as small as that from the CMB. However, we note that it does depend on the drag scale r_d calibrated from the CMB so it is not an entirely independent measurement.

4 CONCLUSIONS

We have used the recent DES supernova data (DES Collaboration 2024) calibrated by the recent DESI BAO measurements (DESI Collaboration 2024) to measure an 'inverse distance ladder' estimation of $H_0 = 67.19^{+0.66}_{-0.64}$ km s^{-1} Mpc^{-1}. The uncertainties on our H_0 measurement are ~ 50 per cent smaller than the inverse distance ladder measurement using the DES 3 yr sample (Macaulay et al. 2019) and comparable with the Planck measurement. Interestingly, while our value of H_0 agrees with the best-fitting Planck H_0 value in flat-ΛCDM, the expansion history differs substantially from that of the best-fitting Planck model (see Figs 1 and 2). This reflects the fact that DES and DESI both prefer a time-varying equation of state of dark energy, w, over a cosmological constant. Alternatively, it remains important to consider that there might be an unexposed systematic error. This motivates the efforts to continue acquiring more and better data to investigate these cosmological tensions further.

Software : NUMPY (Harris et al. 2020), ASTROPY (Astropy Collaboration 2013, 2018), MATPLOTLIB (Hunter 2007), PANDAS (pandas development team 2020), SCIPY (Virtanen et al. 2020), CHAINCONSUMER (Hinton 2016), DYNESTY (Skilling 2004; Skilling 2006; Higson et al. 2018; Speagle 2020; Koposov et al. 2023).

DATA AVAILABILITY

The DYNESTY chains, along with a basic script to replicate the results presented in Table 1, can be found at https://github.com/RyanCamo/inversedistanceladder/.

REFERENCES

Abbott T. M. C., et al., 2019, ApJ, 872, L30

Aghanim N., et al., 2020, A&A, 641, A6

Akaike H., 1974, IEEE Trans. Autom. Control, 19, 716

Alam S., et al., 2017, MNRAS, 470, 2617

Anand G. S., Tully R. B., Rizzi L., Riess A. G., Yuan W., 2022, ApJ, 932, 15

Anderson L., et al., 2014, MNRAS, 441, 24

Astropy Collaboration, 2013, A&A, 558, A33

Astropy Collaboration, 2018, AJ, 156, 123

Aubourg É. et al., 2015, Phys. Rev. D, 92, 123516

Aylor K., Joy M., Knox L., Millea M., Raghunathan S., Wu W. L. K., 2019, ApJ, 874, 4

Betoule M., et al., 2014, A&A, 568, A22

Biscardi I., Raimondo G., Cantiello M., Brocato E., 2008, ApJ, 678, 168

Blake C., Glazebrook K., 2003, ApJ, 594, 665

Blake C. et al., 2011, MNRAS, 418, 1725

Blakeslee J. P., Ajhar E. A., Tonry J. L., 1999, in Heck A., Caputo F., eds, Distances from Surface Brightness Fluctuations. Springer Netherlands, Dordrecht, p. 181,

Blakeslee J. P. et al., 2009, ApJ, 694, 556

Brout D. et al., 2022, ApJ, 938, 110

Camarena D., Marra V., 2020, MNRAS, 495, 2630

Camarena D., Marra V., 2023, The tension in the absolute magnitude of Type Ia supernovae. preprint (arXiv:2307.02434)

Camilleri R., et al., 2024, MNRAS, 533, 2615

Carter P., Beutler F., Percival W. J., Blake C., Koda J., Ross A. J., 2018, MNRAS, 481, 2371

DES Collaboration et al., 2024, ApJ, 973, L14

DESI Collaboration, 2024, DESI 2024 VI: Cosmological Constraints from the Measurements of Baryon Acoustic Oscillations, preprint (arXiv:2404.03002)

Dam L. H., Heinesen A., Wiltshire D. L., 2017, MNRAS, 472, 835

Dinda B. R., Banerjee N., 2023, Phys. Rev. D, 107, 063513

Etherington I., 1933, The Lond. Edinburgh Dublin Philos. Mag. J. Sci., 15, 761

Freedman W. L., 2021, ApJ, 919, 16

Garnavich P., et al., 2023, ApJ, 953, 35

Harris C. R., et al., 2020, Nature, 585, 357

Higson E., Handley W., Hobson M., Lasenby A., 2018, Stat. Comput., 29, 891

Hinton S. R., 2016, J. Open Source Softw., 1, 00045

Hunter J. D., 2007, Comput. in Sci. and Eng., 9, 90

Khetan N., et al., 2021, A&A, 647, A72

Koposov S., et al., 2023, joshspeagle/dynesty: v2.1.3. https://doi.org/10.5281/zenodo.8408702

Lemos P., Lewis A., 2023, Phys. Rev. D, 107, 103505

Li S., Beaton R. L., 2024, The Tip of the Red Giant Branch Distance Ladder and the Hubble Constant, preprint (arXiv:2403.17048)

Linder E. V., 2003, Phys. Rev. D, 68, 083504

Macaulay E., et al., 2019, MNRAS, 486, 2184

McDonald P., Eisenstein D. J., 2007, Phys. Rev. D, 76 063009

Möller A., et al., 2022, MNRAS, 514, 5159

Mukherjee P., Sen A. A., 2024, Model-independent cosmological inference post DESI DR1 BAO measurements, preprint (arXiv:2405.19178, https://arxiv.org/abs/2405.19178)

pandas development team T., 2020, pandas-dev/pandas: Pandas, https://doi.org/10.5281/zenodo.3509134

Riess A. G., et al., 2022, ApJ, 934, L7

Sánchez B. O., et al., 2024, ApJ, 975, 5

Scolnic D., et al., 2022, ApJ, 938, 113

Scolnic D., et al., 2023, ApJ, 954, L31

Seo H.-J., Eisenstein D. J., 2003, ApJ, 598, 720

Shah P., Lemos P., Lahav O., 2021, A&AR, 29, 9

Skilling J., 2004, in Fischer R., Preuss R., Toussaint U. V.eds, AIP Conf. Proc. Vol. 735, Bayesian Inference and Maximum Entropy Methods in Science and Engineering: 24th International Workshop on Bayesian Inference and Maximum Entropy Methods in Science and Engineering. Am. Inst. Phys, New York, p. 395,

Skilling J., 2006, Bayesian Anal., 1, 833

Speagle J. S., 2020, MNRAS, 493, 3132

Tonry J., Schneider D. P., 1988, AJ, 96, 807

Trotta R., 2008, Contemp. Phys., 49, 71

Vincenzi M., et al., 2024, ApJ, 975, 86

Virtanen P., et al., 2020, Nat. Methods, 17, 261

Visser M., 2004, Class. Quantum Gravity, 21, 2603

Zhang M.-J., Li H., Xia J.-Q., 2017, Eur. Phys. J. C, 77, 434

[1] *School of Mathematics and Physics, University of Queensland, Brisbane, QLD 4072, Australia*

[2] *The Research School of Astronomy and Astrophysics, Australian National University, ACT 2601, Australia*

[3] *Center for Astrophysics, Harvard and Smithsonian, 60 Garden Street, Cambridge, MA 02138, USA*

[4] *Institut d'Estudis Espacials de Catalunya (IEEC), E-08034 Barcelona, Spain*

[5] *Institute of Space Sciences (ICE, CSIC), Campus UAB, Carrer de Can Magrans, s/n, E-08193 Barcelona, Spain*

[6] *Centre for Astrophysics and Supercomputing, Swinburne University of Technology, VIC 3122, Australia*

[7] *Department of Physics and Astronomy, University of Pennsylvania, Philadelphia, PA 19104, USA*

[8] *Centre for Gravitational Astrophysics, College of Science, The Australian National University, ACT 2601, Australia*

[9] *School of Mathematics and Physics, University of Surrey, Guildford, Surrey GU2 7XH, UK*

[10] *Department of Physics, Duke University Durham, NC 27708, USA*

[11] *Department of Physics and Astronomy, University College London, Gower Street, London WC1E 6BT, UK*

[12] *School of Physics and Astronomy, University of Southampton, Southampton SO17 1BJ, UK*

[13] *Université Grenoble Alpes, CNRS, LPSC-IN2P3, F-38000 Grenoble, France*

[14] *Fermi National Accelerator Laboratory, P. O. Box 500, Batavia, IL 60510, USA*

[15] *Cerro Tololo Inter-American Observatory, NSF's National Optical-Infrared Astronomy Research Laboratory, Casilla 603, La Serena, Chile*

[16] *Laboratório Interinstitucional de e-Astronomia – LIneA, Rua Gal. José Cristino 77, Rio de Janeiro, RJ – 20921-400, Brazil*

[17] *Department of Physics, University of Michigan, Ann Arbor, MI 48109, USA*

[18] *Departamento de Física Teórica and IPARCOS, Universidad Complutense de Madrid, E-28040 Madrid, Spain*

[19] *Institut de Física d'Altes Energies (IFAE), The Barcelona Institute of Science and Technology, Campus UAB, E-08193 Bellaterra (Barcelona), Spain*

[20] *Institute of Cosmology and Gravitation, University of Portsmouth, Portsmouth PO1 3FX, UK*

[21] *Physics Department, 2320 Chamberlin Hall, University of Wisconsin-Madison, 1150 University Avenue Madison, WI 53706-1390, USA*

[22] *University Observatory, Faculty of Physics, Ludwig-Maximilians-Universität, Scheinerstr. 1, D-81679 Munich, Germany*

[23] *Department of Astronomy and Astrophysics, University of Chicago, Chicago, IL 60637, USA*

[24] *Kavli Institute for Particle Astrophysics and Cosmology, P. O. Box 2450, Stanford University, Stanford, CA 94305, USA*

[25] *SLAC National Accelerator Laboratory, Menlo Park, CA 94025, USA*

[26] *Instituto de Astrofísica de Canarias, E-38205 La Laguna, Tenerife, Spain*

[27] *INAF-Osservatorio Astronomico di Trieste, via G. B. Tiepolo 11, I-34143 Trieste, Italy*

[28] *Jodrell Bank Center for Astrophysics, School of Physics and Astronomy, University of Manchester, Oxford Road, Manchester M13 9PL, UK*

[29] *School of Physics and Astronomy, University of Nottingham, Nottingham NG7 2RD, UK*

[30] *Hamburger Sternwarte, Universität Hamburg, Gojenbergsweg 112, D-21029 Hamburg, Germany*

[31] *Department of Physics, IIT Hyderabad, Kandi, Telangana 502285, India*

[32] *Jet Propulsion Laboratory, California Institute of Technology, 4800 Oak Grove Dr, Pasadena, CA 91109, USA*

[33] *Institute of Theoretical Astrophysics, University of Oslo. P.O. Box 1029 Blindern, NO-0315 Oslo, Norway*

[34] *Kavli Institute for Cosmological Physics, University of Chicago, Chicago, IL 60637, USA*

[35] *Instituto de Fisica Teorica UAM/CSIC, Universidad Autonoma de Madrid, E-28049 Madrid, Spain*

[36] *Center for Astrophysical Surveys, National Center for Supercomputing Applications, 1205 West Clark St., Urbana, IL 61801, USA*

[37] *Department of Astronomy, University of Illinois at Urbana-Champaign, 1002 W. Green Street, Urbana, IL 61801, USA*

[38] *Santa Cruz Institute for Particle Physics, Santa Cruz, CA 95064, USA*

[39] *Center for Cosmology and Astro-Particle Physics, The Ohio State University, Columbus, OH 43210, USA*

[40] *Department of Physics, The Ohio State University, Columbus, OH 43210, USA*

[41] *Australian Astronomical Optics, Macquarie University, North Ryde, NSW 2113, Australia*

[42] *Lowell Observatory, 1400 Mars Hill Rd, Flagstaff, AZ 86001, USA*

[43] *Sydney Institute for Astronomy, School of Physics, A28, The University of Sydney, NSW 2006, Australia*

[44] *Departamento de Física Matemática, Instituto de Física, Universidade de São Paulo, CP 66318, São Paulo, SP 05314-970, Brazil*

[45] *George P. and Cynthia Woods Mitchell Institute for Fundamental Physics and Astronomy, and Department of Physics and Astronomy, Texas A&M University, College Station, TX 77843, USA*

[46] *LPSC Grenoble – 53, Avenue des Martyrs, F-38026 Grenoble, France*

[47] *Institució Catalana de Recerca i Estudis Avançats, E-08010 Barcelona, Spain*

[48] *Department of Astrophysical Sciences, Princeton University, Peyton Hall, Princeton, NJ 08544, USA*

[49] *Observatório Nacional, Rua Gal. José Cristino 77, Rio de Janeiro, RJ – 20921-400, Brazil*

[50] *Department of Physics, Carnegie Mellon University, Pittsburgh, PA 15312, USA*

[51] *Department of Physics and Astronomy, Pevensey Building, University of Sussex, Brighton BN1 9QH, UK*

[52] *Department of Physics, Northeastern University, Boston, MA 02115, USA*

[53] *Centro de Investigaciones Energéticas, Medioambientales y Tecnológicas (CIEMAT), 28040 Madrid, Spain*

[54] *Computer Science and Mathematics Division, Oak Ridge National Laboratory, Oak Ridge, TN 37831, USA*

[55] *Department of Astronomy, University of California, Berkeley, 501 Campbell Hall, Berkeley, CA 94720, USA*

[56] *Lawrence Berkeley National Laboratory, 1 Cyclotron Road, Berkeley, CA 94720, USA*

This paper has been typeset from a TEX/LATEX file prepared by the author.